

Evolution of high-Arctic glacial landforms during deglaciation

N.G. Midgley ^{a,*}, T.N. Tonkin ^{a,b}, D.J. Graham ^c, S.J. Cook ^d

^a School of Animal, Rural and Environmental Sciences, Nottingham Trent University, Brackenhurst Campus, Southwell, Nottinghamshire NG25 0AQ, UK

^b Department of Natural Sciences, University of Derby, Kedleston Road, Derby DE22 1GB, UK

^c Polar and Alpine Research Centre, Loughborough University, Leicestershire LE11 3TU, UK

^d School of Social Sciences, University of Dundee, Nethergate, Dundee DD1 4HN, UK

ARTICLE INFO

Article history:

Received 29 November 2017

Received in revised form 27 March 2018

Accepted 28 March 2018

Available online 29 March 2018

Keywords:

Unmanned aerial vehicle (UAV)

Structure-from-motion (SfM)

Ground penetrating radar (GPR)

Ice-cored moraine

Midtre Lovénbreen, Svalbard

ABSTRACT

Glacial landsystems in the high-Arctic have been reported to undergo geomorphological transformation during deglaciation. This research evaluates moraine evolution over a decadal timescale at Midtre Lovénbreen, Svalbard. This work is of interest because glacial landforms developed in Svalbard have been used as an analogue for landforms developed during Pleistocene mid-latitude glaciation. Ground penetrating radar was used to investigate the subsurface characteristics of moraines. To determine surface change, a LiDAR topographic data set (obtained 2003) and a UAV-derived (obtained 2014) digital surface model processed using structure-from-motion (SfM) are also compared. Evaluation of these data sets together enables subsurface character and landform response to climatic amelioration to be linked. Ground penetrating radar evidence shows that the moraine substrate at Midtre Lovénbreen includes ice-rich (radar velocities of 0.17 m ns^{-1}) and debris-rich (radar velocities of $0.1\text{--}0.13 \text{ m ns}^{-1}$) zones. The ice-rich zones are demonstrated to exhibit relatively high rates of surface change (mean thresholded rate of -4.39 m over the 11-year observation period). However, the debris-rich zones show a relatively low rate of surface change (mean thresholded rate of -0.98 m over the 11-year observation period), and the morphology of the debris-rich landforms appear stable over the observation period. A complex response of proglacial landforms to climatic warming is shown to occur within and between glacier forelands as indicated by spatially variable surface lowering rates. Landform response is controlled by the ice-debris balance of the moraine substrate, along with the topographic context (such as the influence of meltwater). Site-specific characteristics such as surface debris thickness and glaciofluvial drainage are, therefore, argued to be a highly important control on surface evolution in ice-cored terrain, resulting in a diverse response of high-Arctic glacial landsystems to climatic amelioration. These results highlight that care is needed when assessing the long-term preservation potential of contemporary landforms at high-Arctic glaciers. A better understanding of ice-cored terrain facilitates the development of appropriate age and climatic interpretations that can be obtained from palaeo ice-marginal landsystems.

© 2018 The Authors. Published by Elsevier B.V. This is an open access article under the CC BY-NC-ND license (<http://creativecommons.org/licenses/by-nc-nd/4.0/>).

1. Introduction

The aim of this research is to investigate the geomorphological evolution of proglacial landforms during deglaciation in Svalbard. To achieve this aim, data were collected — at Midtre Lovénbreen, Svalbard (Fig. 1) — using a range of techniques, including (i) ground penetrating radar (GPR) data collected in 2009 to assess moraine structure and composition; (ii) archive aerial imagery and LiDAR data, both acquired in 2003; and (iii) aerial imagery acquired in 2014 using an unmanned aerial vehicle (UAV) to assess any change in moraine morphology over the 11-year period from 2003. This research also provides the opportunity to contrast landform dynamics at adjacent glaciers with similar glacio-logical conditions, following recent investigation of landforms at

neighbouring Austre Lovénbreen (Midgley et al., 2013; Tonkin et al., 2016).

Neoglacial moraines in Svalbard have been used as analogues for Pleistocene moraines in the mid-latitudes (e.g., Hambrey et al., 1997; Bennett et al., 1998; Graham and Midgley, 2000); however, many contain buried ice (e.g., Bennett et al., 1996, 2000; Lyså and Lønne, 2001; Sletten et al., 2001; Lønne and Lyså, 2005; Schomacker and Kjær, 2008; Evans, 2009; Midgley et al., 2013; Ewertowski, 2014; Ewertowski and Tomczyk, 2015; Tonkin et al., 2016), which means that there is potential for significant landform change associated with the ablation of buried ice. The validity of such analogues relies upon a lack of buried ice in the proglacial area in order for the landforms to be preserved through a period of complete deglaciation. Consequently, the extent to which Neoglacial moraines in Svalbard serve as Pleistocene analogues has been subject to debate (e.g., Lukas, 2005, 2007; Graham et al., 2007).

* Corresponding author.

E-mail address: nicholas.midgley@ntu.ac.uk (N.G. Midgley).

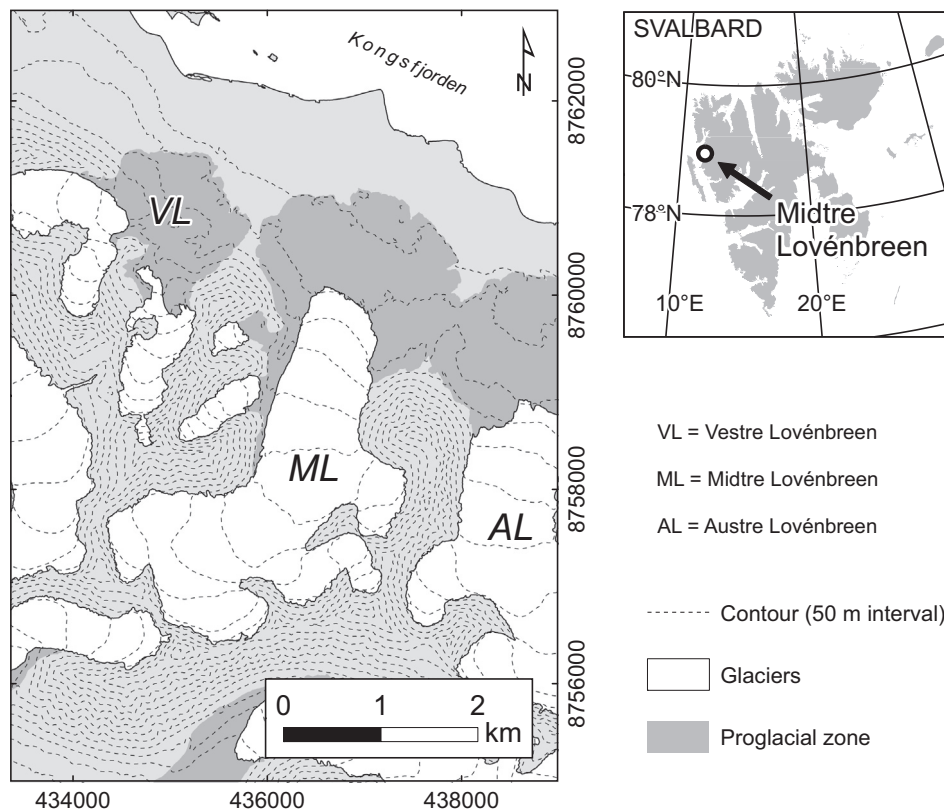


Fig. 1. Study site location. (A) Midtre Lovénbreen on Svalbard in the Norwegian high-Arctic. (B) Midtre Lovénbreen on Brøggerhalvøya near Ny-Ålesund. Data from the Norwegian Polar Institute (2014).

Globally, paraglacial processes (e.g., Church and Ryder, 1972; Ballantyne, 2002) are responsible for remobilising glacial sediment in proglacial areas during and following deglaciation (Knight and Harrison, 2009; Fame et al., 2018). Moraine slopes in proglacial areas may adjust rapidly following deglaciation (e.g., Sharp, 1984; Curry, 1999; Curry et al., 2006). In polar regions characterised by the presence of permafrost, rates of landsystem transformation are often expedited by the disintegration of buried ice (Fitzsimons, 1996; Bennett et al., 2000; Etienne et al., 2008; Oliva and Ruiz-Fernández, 2015). For example, Mercier et al. (2009) reported that following deglaciation sediment mantled slopes undergo significant transformation, with the formation of gullies controlled by the ablation of buried ice. Conceptual pathways of landsystem evolution predict that upon complete deglaciation, ice-cored terrain will result in a ‘hummocky’ assemblage of landform (Boulton, 1972), although preservation of buried ice is permitted under an extensive sediment mantle. Controls on buried ice ablation were reviewed in Schomacker (2008). Subsequent to the publication of this review, a wider range of studies have provided insight into the processes of buried ice ablation and paraglacial redistribution of sediments following deglaciation (e.g., Irvine-Fynn et al., 2011; Ewertowski, 2014; Ewertowski and Tomczyk, 2015; Tonkin et al., 2016).

At Midtre Lovénbreen, previous work has focused on ice-rich moraine areas with low preservation potential over a 2-year period from 2003 to 2005 (Irvine-Fynn et al., 2011), hinting at the possibility that Svalbard moraines undergo significant transformation during deglaciation, which may last several decades or longer (e.g., Evans, 2009; Ewertowski and Tomczyk, 2015). In this study, observations on moraine transformation are extended beyond the 2-year study period previously reported (Irvine-Fynn et al., 2011) to facilitate understanding of the evolution of high-Arctic glacial landforms on a decadal scale through the use of high-resolution LiDAR and UAV-SfM (structure-from-motion) derived topographic data sets (techniques demonstrated to be of value in glacial environments by Bhardwaj et al., 2016a, 2016b). The

burial and long-term preservation of relict ice is of interest as a potential palaeoglaciological and palaeoenvironmental archive (e.g., Sugden et al., 1995; Schäfer et al., 2000; Murton et al., 2005; Waller et al., 2012). In addition, understanding the preservation history of buried ice will also assist with appropriate landform age determination (e.g., Kirkbride and Winkler, 2012; Çiner et al., 2015; Tonkin et al., 2017; Crump et al., 2017) and assist with former glacier reconstruction (e.g., Benn and Hulton, 2010; Pellitero et al., 2016). This work is important because it advances our understanding of the buried ice ablation process by providing insight into the deglaciation dynamics of a high-Arctic glacier foreland over a decadal timescale and it contributes to our knowledge of how debris-covered cryospheric systems respond to ameliorating climatic conditions.

2. Study site

Midtre Lovénbreen is a small valley glacier (currently ca. 4 km in length, but ca. 5 km in length at the Neoglacial maximum) located in the Norwegian high-Arctic (terminus ca. 78° 53.7' N 12° 3.5' E) around 4 km to the SE of Ny-Ålesund (Fig. 1). An arcuate moraine complex shows that the glacier has receded by around 1 km since the Neoglacial maximum (Fig. 2). Svalbard had 38,871 km² of glacier area at the Neoglacial maximum and this has now decreased by 13.1% (Martín-Moreno et al., 2017). Midtre Lovénbreen has a long mass balance record dating back to 1968, with currently published data to 2015 (WGMS, 2017). These data demonstrate a mean mass balance of -0.39 m water equivalent over the record period, with only 5 years showing a positive annual balance. The west coast of Spitsbergen is warmed by the West Spitsbergen Current and experiences a relatively mild climate for its latitude. Ny-Ålesund (79° N) experienced a mean annual temperature of -6.3 °C from 1961 to 1990, -5.2 °C from 1981 to 2010 (Førland et al., 2011), -4.4 °C from 1979 to 2014 (Osuch and Wawrzyniak,

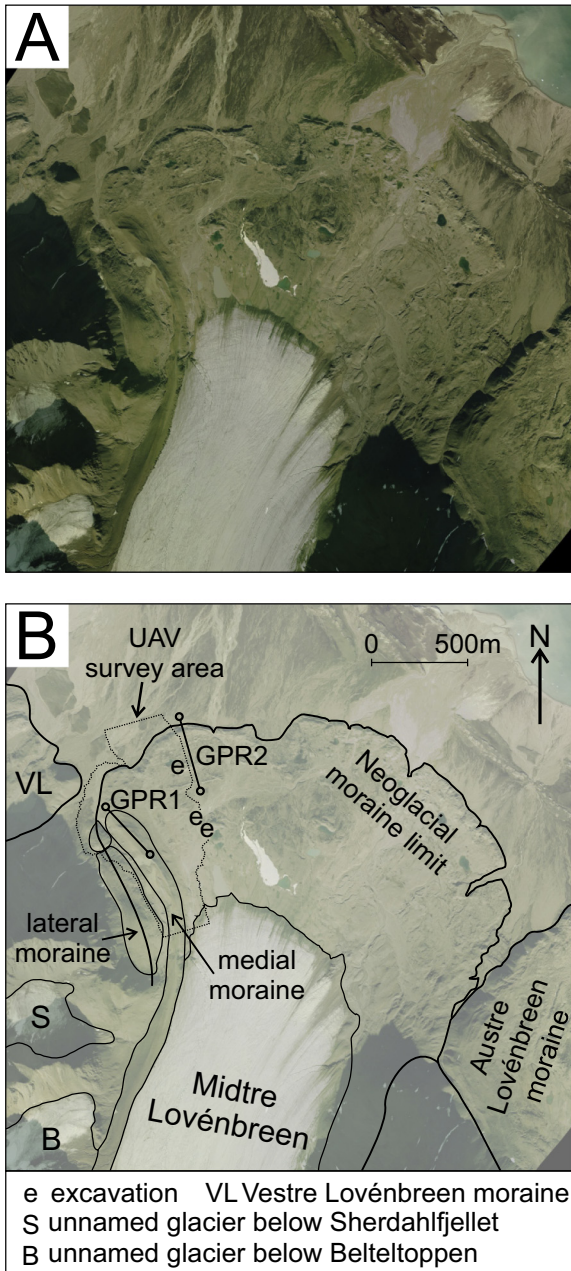


Fig. 2. Geomorphological interpretation of Midtre Lovénbreen and the glacier foreland. (A) Aerial orthomosaic imagery (from summer 2003) of the terminus of Midtre Lovénbreen and the proglacial area (aerial data are from the UK Natural Environment Research Council (NERC) Airborne Research and Survey Facility (ARSF) that are provided courtesy of NERC via the NERC Earth Observation Data Centre); (B) summary map of the area covered in part A with relevant features outlined, area surveyed by UAV in 2014 delimited, and ground penetrating radar transect locations identified (GPR1 and GPR2).

2017), and -3.8°C from 2003 to 2014 (data from the Norwegian Meteorological Institute downloaded via eKlima web portal).

The likely maximum Neoglacial extent of Midtre Lovénbreen was photographed by Axel Hamberg in 1892 CE (Hamberg, 1894; picture reproduced by Hambrey et al., 2005), mapped by Isachsen in 1906–1907 CE (Isachsen, 1912), photographed by Sigvald Moa in spring 1918 CE (Fig. 3) (picture reproduced by Hanoa, 1993), and also photographed by W. Mittelholzer in 1923 (De Geer, 1930). Midtre Lovénbreen exhibits a near-vertical ice-margin at the outer-frontal moraine in 1892 CE and 1918 CE (Hamberg, 1894; Hanoa, 1993). A number of englacial debris bands are shown in the 1918 CE ice margin image and are comparable to the debris bands that were also identified by

Hambrey et al. (2005) on the 1892 CE image. By 1936 CE, Norwegian Polar Institute oblique aerial imagery shows that the glacier margin had receded from its Neoglacial maximum and thinned significantly to form a low-angle slope (Fig. 4; also see Midgley and Tonkin, 2017). The thermal regime of Midtre Lovénbreen has previously been reported to be polythermal (Björnsson et al., 1996), but the warm-based zone has reduced and the cold-based zone has increased in extent during the twentieth century (Hambrey et al., 2005).

The whole moraine complex at Midtre Lovénbreen broadly comprises four components. Component 1: Lateral moraines that extended along the sides of Midtre Lovénbreen at its Neoglacial maximum extent. Component 2: A medial moraine located in the zone separating flow between the main flow unit of Midtre Lovénbreen and a former tributary. The former tributary to the northeast of Berteltoppen is an unnamed glacier that separated from the rest of Midtre Lovénbreen sometime between 1948 and 1966, based upon surface structural interpretation of aerial images by Hambrey et al. (2005). Potential, although unlikely, contribution to this flow unit may also have come from an unnamed glacier to the south of Sherdahlfjellet shown on 1936 aerial imagery (Fig. 4). By 2003 the medial moraine appears to be a relict feature that now marks the lateral edge of Midtre Lovénbreen. Component 3: An arcuate outer-frontal moraine marking the Neoglacial maximum extent of Midtre Lovénbreen. Component 4: Comparatively low-relief ‘hummocky moraine’ within the moraine-mound complex.

3. Methods

3.1. Subsurface characterisation

Ground penetrating radar has been shown to provide useful information on subsurface composition and structure in glacial and proglacial settings (e.g., Bennett et al., 2004; Lukas and Sass, 2011; Midgley et al., 2013; Tonkin et al., 2017). In this study, a pulseEKKO Pro ground penetrating radar (GPR) system was used with 100 MHz centre frequency antennae to investigate the subsurface moraine characteristics along two transects oriented parallel to inferred former ice flow direction (Fig. 2B). This resulted in transect GPR1 being undertaken parallel to the moraine crest orientation, whereas GPR2 was transverse to the crest orientation. The GPR data sets were collected during winter conditions to avoid the presence of liquid water, thus maximising penetration and minimising signal attenuation. Antennae were stepped at 0.25-m intervals, with 1-m separation and a perpendicular broadside configuration. Each trace was manually triggered, positioned along a 100-m tape with a 750–1000 ns time window and 36 stacks. The GPR control unit was positioned at least 5 m away from the transmitter and receiver to minimise signal interference. Change in topography along each transect was surveyed using an automatic level. Radar velocities were obtained by matching hyperbolas to point diffractions in the substrate (e.g., a technique previously applied to ice-cored terrain by Brandt et al., 2007). The derived velocities were used to indicate subsurface composition.

Analysis of buried ice was undertaken within three shallow trenches, of up to 5 m length, along transect GPR1. Samples of ice were retrieved and described after having first removed the top 20–30 cm of ice, following the procedures outlined by Toubes-Rodrigo et al. (2016).

3.2. Surface characterisation: 2003

Aerial photographs and LiDAR data were collected on 9 August 2003 by the UK Natural Environment Research Council (NERC) Airborne Research and Survey Facility (ARSF) and downloaded via the NERC Earth Observation Data Centre (NEODC). The Agisoft Photoscan image processing and 2003 orthomosaic production was generated using the workflow documented in Midgley and Tonkin (2017). The LiDAR data were collected using an Optech ALTM3033 laser scanner at an aircraft

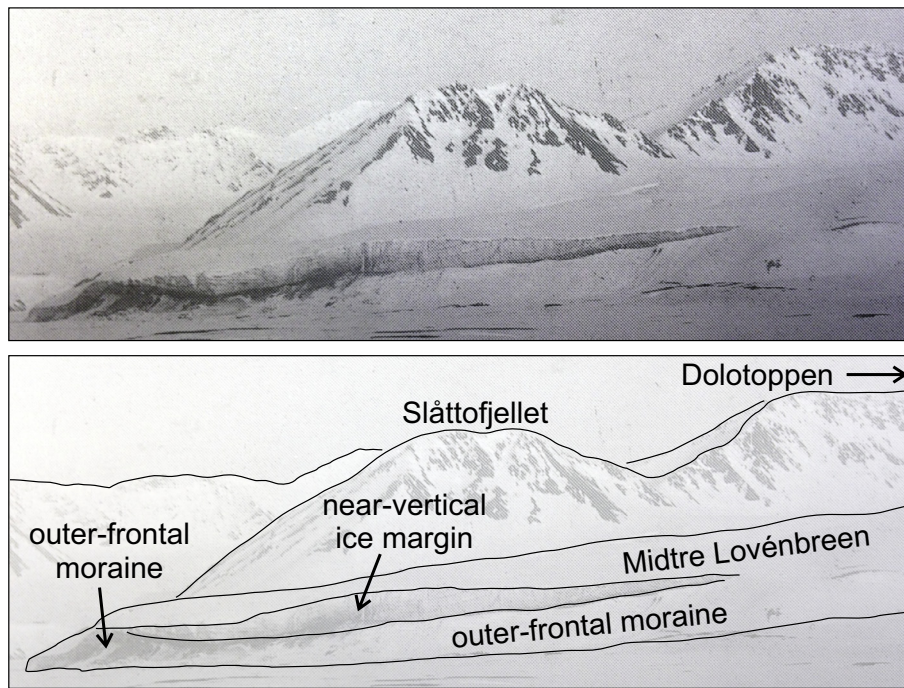


Fig. 3. Historic image of Midtre Lovénbreen taken in spring 1918 with key elements delimited. (adapted from Hanoa, 1993).

ground speed of ca. 77 ms^{-1} and mean altitude of 1600 m asl. This resulted in a resolution of around 1.1 points/m^2 over the proglacial area (Irvine-Fynn et al., 2011). A DEM of the area of interest was produced at 2 m/pixel resolution (e.g., Arnold et al., 2006) using linear interpolation.

3.3. Surface characterisation: 2014

The SfM photogrammetry, with imagery typically obtained using small UAVs, is now commonplace for low-level aerial image acquisition (e.g., Tonkin et al., 2014; Rippin et al., 2015; Ely et al., 2017; Rossini et al., 2018). At Midtre Lovénbreen, a DJI S800 UAV was used to acquire aerial images on 20 July 2014. A total of six flights, each 13 to 15 min in duration, with mean flight altitude of 110 m were undertaken in the area of interest. A consumer-grade compact mirrorless camera (Canon EOS M) with 18 MP resolution was used to obtain the images using an internal intervalometer that resulted in an image being obtained approximately every 5 s during each flight. Agisoft Photoscan was used to process a total of 1042 images with 17 ground-control points (GCPs). The same Agisoft Photoscan image processing workflow that was used with the 2003 aerial images was also used for the 2014 UAV imagery (workflow described by Midgley and Tonkin, 2017). The GCPs were marked on the ground using A4-sized targets that were surveyed with a Leica 1200 dGPS. The SfM processing of the UAV-derived imagery provided an image resolution of 2.08 cm/pixel and a point cloud with 112.3 million points over the survey area, resulting in a resolution of around 12.5 points/m^2 (an order of magnitude greater than the LiDAR resolution).

3.4. Surface change detection: 2003–2014

The 2014 UAV-derived DEM was compared to the 2003 LiDAR-derived DEM for the purpose of assessing surface evolution over this time period. The 2014 SfM DEM was resampled to the same resolution as the LiDAR-derived DEM (2 m/pixel) to facilitate comparison between the data sets. The 2.5D difference between the two data sets was

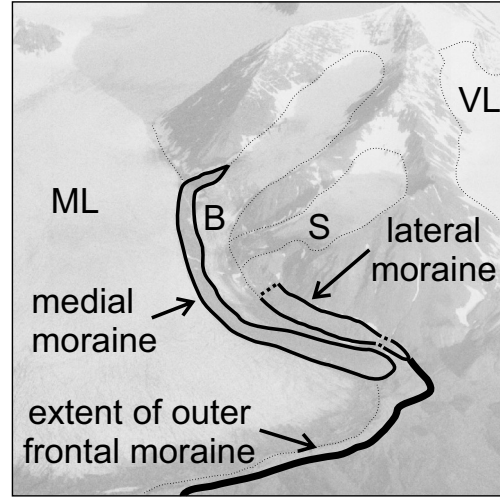
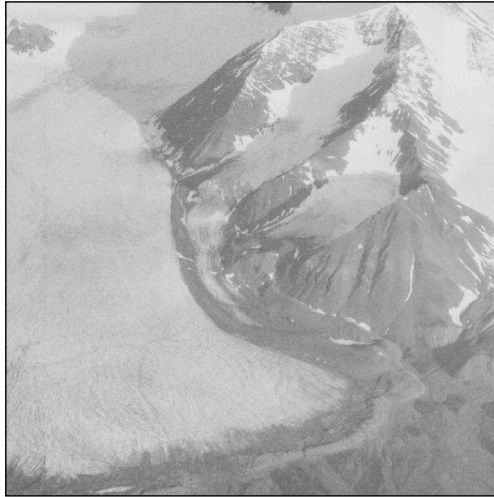
calculated by subtraction, and the resulting data subjected to error thresholding using the Geomorphologic Change Detection plugin for ArcGIS by Wheaton et al. (2010). Arnold et al. (2006) estimated that the RMS (root mean square) error in the study area may exceed 0.2 m for the LiDAR data. The 2014 SfM DEM is likely to represent a highly accurate representation of the terrain (e.g., Tonkin et al., 2016) with the resulting data well fitted to the 17 GCPs, providing a total RMSE value of 0.052 m. Using a 0.2-m error value for the 2003 LiDAR DEM and a 0.05-m error value for the 2014 UAV DEM, a propagated error (after Brasington et al., 2003) of 0.21 m is found. Using the survey setup described above minor elevation errors are expected in areas of the 2014 SfM DEM not subject to ground control (e.g., Tonkin and Midgley, 2016). To avoid potentially spurious results, data located in excess of 100 m from the nearest GCP on the final DEM of Difference were removed (Tonkin and Midgley, 2016).

4. Results

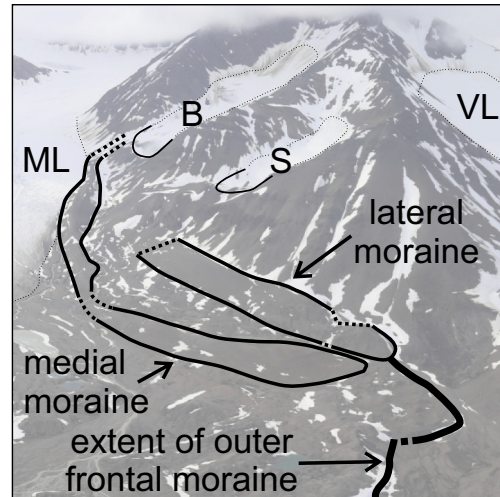
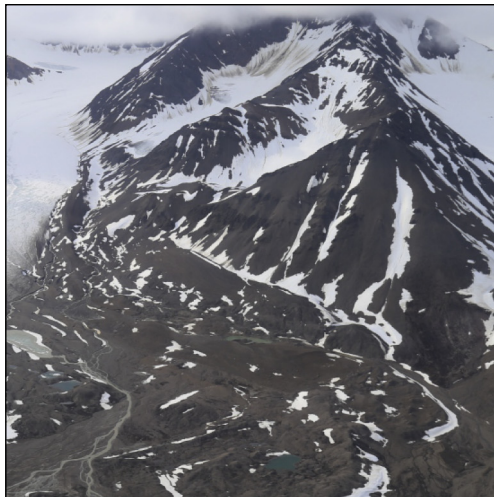
4.1. Subsurface characterisation

Within transect GPR1, three substrate zones are identified: substrate zone 1 at 0–295 m; substrate zone 2 at 295–340 m; and substrate zone 3 at 340 m onward (Fig. 5). Substrate zone 1 (0–295 m) has numerous up-glacier dipping reflectors with a high-density stacked appearance between 0 and 25 m. A number of pronounced asymptotic-style up-glacier dipping reflectors are also found, including one that extends from around 15 m depth at 120 m to intersecting the surface at 215 m. This zone has a low density of point diffractions but is sufficient to enable assessment of subsurface velocity at 0.17 m ns^{-1} ($n 10$). The substrate in this zone also has low signal attenuation and typically returns reflectors from up to 15 m depth and, in places, down to 20 m depth. A shallow trench, excavated along the transect line, had a surface debris layer thickness of ca. 0.25 m, consisting of an upper layer of coarse angular gravel and a lower layer of coarse angular gravel mixed with a mud-rich matrix. Buried ice below the debris layer from 20 m and 215–220

1936



2014



B - unnamed glacier below Belteltoppen ML - Midtre Lovénbreen
 S - unnamed glacier below Sherdahlfjellet VL - Vestre Lovénbreen

Fig. 4. Oblique aerial imagery obtained in approximately similar flight positions showing Midtre Lovénbreen in 1936 and 2014 (the 1936 image is part of aerial photograph S36 1552, published with permission of the Norwegian Polar Institute).

m along the transect is characterised by alternating layers of sediment and clean ice on the scale of millimetres to centimetres in thickness. Included sediment ranges from clay/silt-size particles to centimetre-sized clasts that are angular in nature. The clean ice between debris-bearing layers is occasionally bubble-free, but millimetre-scale bubbles are widespread within the clean and debris-bearing ice layers. Ice from 209 m along the transect is characterised by coarse, bubbly ice. Zone 2 (295–340 m) lacks clear reflectors but has numerous overlapping point diffractions that indicate a velocity of 0.14 m ns^{-1} ($n 4$) and has low signal attenuation. Zone 3 (340–360 m) is characterised by high signal attenuation, lacks clear reflectors, and has velocity characteristics of 0.11 to 0.13 m ns^{-1} ($n 4$).

Within transect GPR2, two substrate zones are identified: substrate zone 1 at 0–330 m; and substrate zone 2 at 330 m onward (Fig. 6). Substrate zone 1 (0–330 m) includes a range of reflector styles, up-glacier

and down-glacier dipping. Analysis of the point diffractions shows substrate velocity characteristics of 0.10 to 0.12 m ns^{-1} ($n 4$). Typically, reflectors from up to 7.5 m depth are found, although a prominent continuous reflector is found within the outer ridge that is at 10-m depth below the ridge crest. Overall, the substrate demonstrates high signal attenuation. The moraine composition along this area of the transect has been described in detail by Midgley et al. (2007). Moraine composition, based upon seven excavated sections each typically around 1 m deep, comprises a number of facies types: diamicton ($n 22$), sandy gravel ($n 16$) along with sand and mud ($n 6$) (Midgley et al., 2007). A single excavation in this area revealed the presence of a buried ice facies at 1.16 m with an ice depth of unknown thickness (Midgley et al., 2007). Subsequent to the publication of Midgley et al. (2007), three further excavations did not reveal any evidence of buried ice within three moraines excavated down to 2.75, 3.0, and 3.3 m. Substrate zone 2 (300–

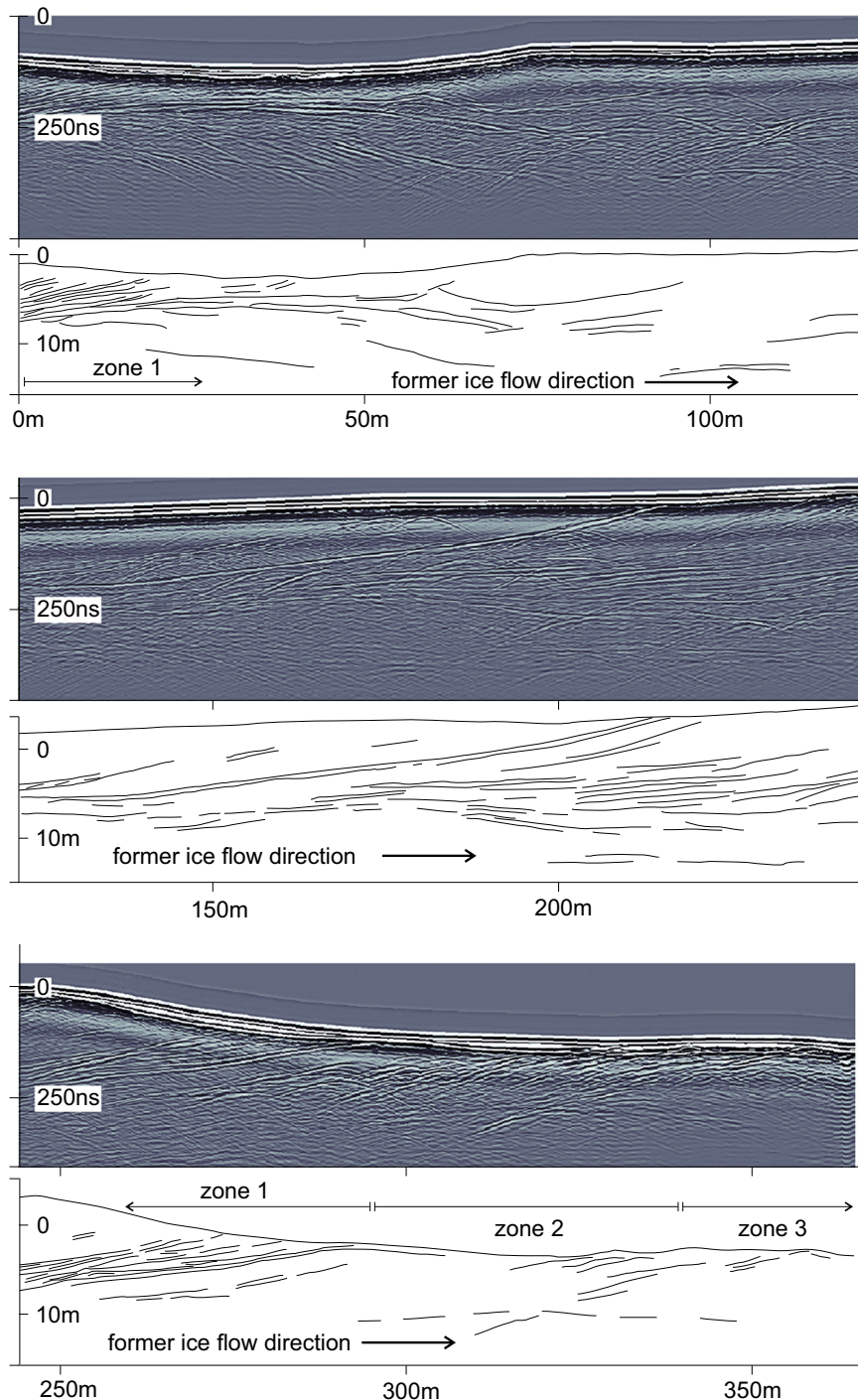


Fig. 5. Ground penetrating radar transect (GPR1) obtained along the medial moraine at Midtre Lovénbreen, Svalbard.

360 m) is characterised by a distinct parallel reflector pattern, no point diffractions, and a high signal attenuation.

4.2. Surface change detection: 2003–2014

In the frontal moraine zone, the mean depth of thresholded surface change was -0.98 m (Table 1) over the observation period. Hummocks, which attain several metres topographic prominence above the frontal moraine surface, show less surface change (Fig. 7). The presence of late-lying snow in the July 2014 survey is the primary cause of areas of positive surface change. This is especially evident when surface change is assessed alongside aerial imagery from the 2014 UAV survey

(Fig. 7), where snow patches are visible at various locations across the study area, especially on the distal slopes of the moraine system.

Within the surveyed lateral moraine zone, a mean thresholded surface change of -0.64 m between 2003 and 2014 was calculated (Table 1). Whilst the amount of change appears to be less (mean surface change) than in the frontal zone, small areas on the landform have lowered by -4 m over the 11-year study period (Figs. 7, 8). Two areas of surface increase were detected in the lateral zone. These relate to (i) the presence of late-lying snow patches in the July 2014 survey; and (ii) geomorphological change associated with sediment redistribution. One area, which is located on the ice-proximal slope of the Neoglacial lateral moraine, is snow free on the 2003 and on the 2014

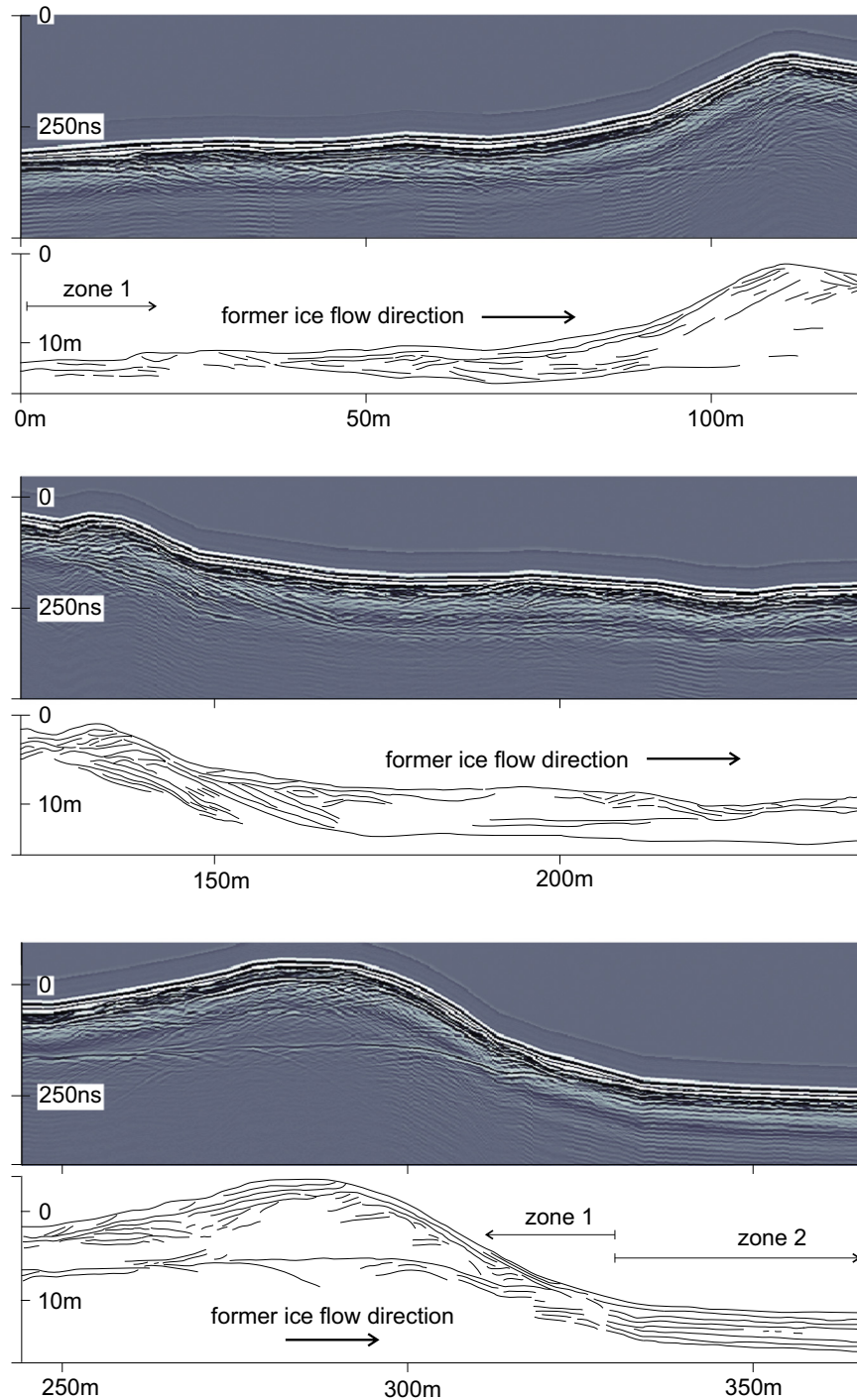


Fig. 6. Ground penetrating radar transect (GPR2) obtained across the frontal moraine at Midtre Lovénbreen, Svalbard.

Table 1
Surface change for the study area segregated into five geomorphological zones.

Zone (as shown in Fig. 7)	Total area assessed (m ²)	Mean depth of surface lowering from 2003 to 2014 (m)		Total thresholded area with detectable change (m ²)	Annual mean thresholded depth of surface lowering between 2003 and 2014 (m)	Total volume of surface lowering from 2003 to 2014 (m ³)	
		Raw	Thresholded			Raw	Thresholded
(i) Frontal	45,508	-0.84	-0.98 (±0.21)	37,304	-0.09	-35,920	-35,080 ± 7528
(ii) Lateral (ice-proximal slope)	23,184	-0.56	-0.64 (±0.21)	18,972	-0.06	-9926	-9603 ± 3133
(iii) Medial	79,440	-4.32	-4.39 (±0.21)	77,760	-0.40	-340,737	-340,564 ± 16,279
(iv) Outwash	3300	-0.22	-0.26 (±0.21)	2160	-0.02	-740	-556 ± 453
(v) Other (glacier foreland)	52,308	-0.25	-0.37 (±0.21)	26,172	-0.03	-11,981	-9211 ± 5189

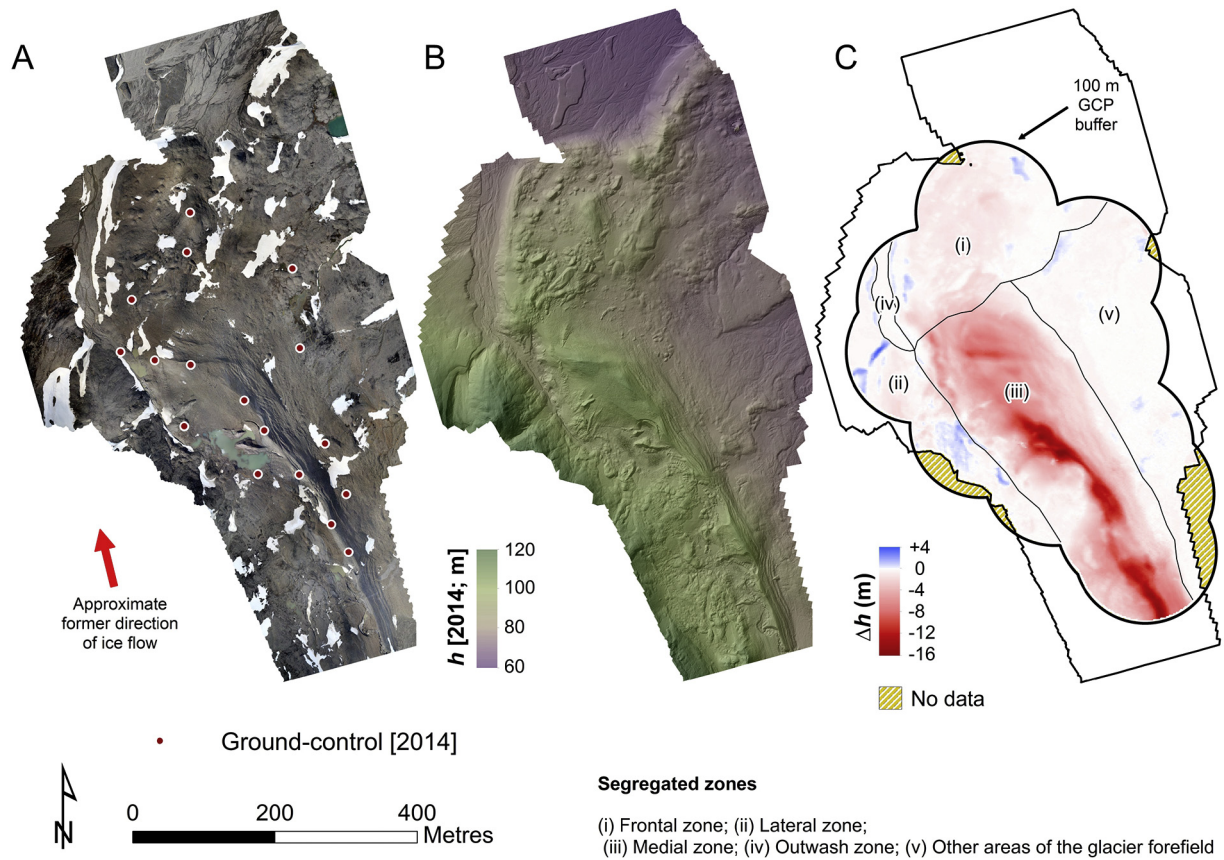


Fig. 7. Analysis of surface evolution from 2003 to 2011. (A) A UAV-derived orthorectified aerial image of the study site and associated ground control applied to the data. (B) A UAV-derived surface model of the survey area obtained in 2014. (C) Surface evolution from 2003 and 2011 obtained by raster differencing. The study area is segregated into five geomorphological zones.

aerial imagery, is located in an area well constrained by ground-control points, and can be confidently related to the redistribution of sediment on the ice-proximal slope of the moraine. This zone shows an increase in surface elevation of up to +1.9 m over the 11-year study period. A range of slope processes may be involved in this sediment redistribution.

The medial moraine zone has the largest surface change, with a mean thresholded depth of surface lowering of -4.39 m (Table 1), which is equivalent to $340,564$ m³ of volume loss from 2003 to 2014. The largest changes over the entire study area were detected on the medial moraine ridge crest and in areas adjacent to standing water, with change exceeding -14 m over the 11-year study period.

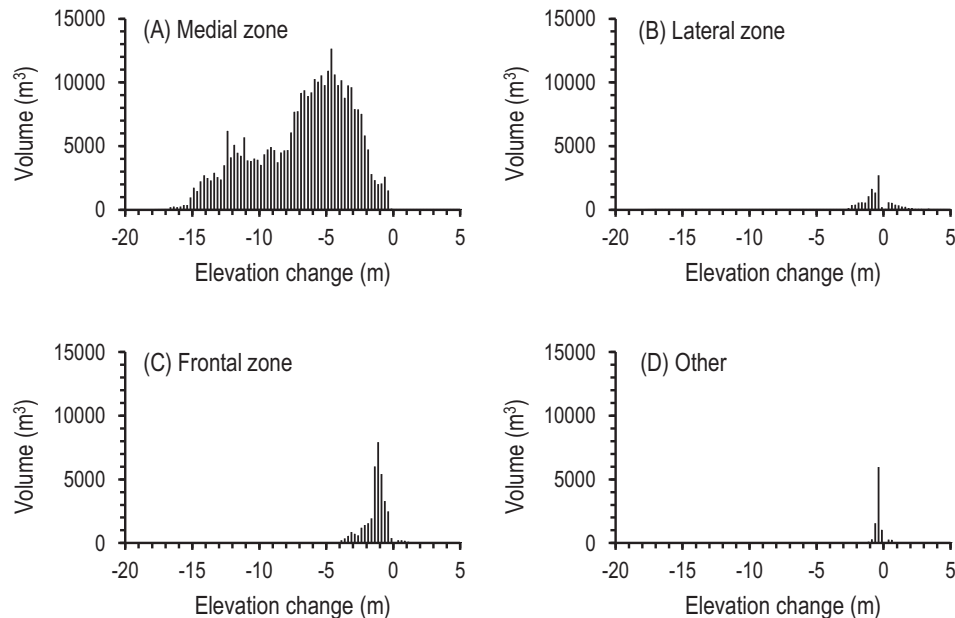


Fig. 8. Histograms of surface change for: (A) the medial moraine; (B) the lateral moraine; (C) the frontal moraine; and (D) other areas of the glacier foreland.

The outwash zone was found to have undergone very limited geomorphological change (-0.26 m thresholded mean surface lowering). Other off-moraine areas of the glacier foreland (see Fig. 7) were also covered by the survey. In this area (ca. $52,000$ m²), a thresholded mean surface change of -0.37 m over the observation period was found.

5. Discussion

5.1. Subsurface characterisation

Within transect GPR1, substrate zone 1 (0–295 m) (Fig. 5), the high radar velocities, low signal attenuation, and trench excavation (revealing a shallow surface debris cover) highlight that the majority of this zone is composed of buried ice. The coarse bubbly ice facies found at 209 m is interpreted as firnified glacier ice. The ice facies found at 20 m and from 215 to 220 m is interpreted as showing rockfall debris entrained at the glacier surface, then buried by further snowfall and firnification. Within substrate zone 2 (295–340 m) (Fig. 5), the lower radar velocities indicate a higher debris concentration within the ice. Within substrate zone 3 (340–360 m) (Fig. 5), the low radar velocities and high signal attenuation indicate a debris-rich substrate. This zone has a high-preservation potential in response to further climatic amelioration and is contiguous with the outer-frontal moraine surveyed along transect GPR2. A similar sequence consisting of an ice-rich zone, transition zone and a debris-rich zone was also recognised at the lateral-frontal moraine of adjacent Austre Lovénbreen (Midgley et al., 2013).

Within transect GPR2, the radar velocities, high signal attenuation, and numerous excavations previously undertaken in the area demonstrate that substrate zone 1 is dominated by a high-debris and low-ice component. Preservation potential, in response to further climatic amelioration, along this transect is high because of the high debris content. Substrate zone 2 covers the proglacial outwash area, beyond the outer moraine marking the Neoglacial maximum. The radar transect in this zone, with parallel reflectors, is a clearly distinguishable radar facies from the moraine found in substrate zone 1. Substrate zone 2 is interpreted as stratified glaciofluvial outwash sediment.

5.2. Surface change detection: 2003–2014

The surface elevation changes documented in this study demonstrate the ablation of buried ice over an 11-year period at this high-Arctic site. The values reported here are similar to studies undertaken at other high-Arctic glaciers (Table 2), where vertical rates of surface lowering up to -1.8 ma⁻¹ have been reported (Schomacker and Kjær, 2008; Irvine-Fynn et al., 2011; Ewertowski, 2014; Ewertowski and Tomczyk, 2015; Tonkin et al., 2016).

Specifically, Irvine-Fynn et al. (2011) reported a surface lowering rate of -0.65 (± 0.2) ma⁻¹ on the 'western lateral moraine' (which is

interpreted as a relict medial moraine in this study) at Midtre Lovénbreen between 2003 and 2005. Over the 11-year study period investigated here, the medial moraine zone had a spatially averaged (mean) change of -4.39 m, which is equivalent to a mean yearly surface change of -0.40 ma⁻¹. However, 4488 m² of the medial moraine zone was found to have lowered at a mean rate exceeding -1 ma⁻¹ over the 11-year study period. The findings indicate the progression of buried ice ablation, resulting in a significant landscape response to climatic amelioration, with some localised areas demonstrating high rates of change and other localised areas demonstrating low rates of change.

The low rates of change that were detected on the frontal moraine system (Table 1) may relate to either (i) stabilised buried ice, below the depth of seasonal thaw, thus permitting limited or negligible rates of ablation (e.g., Etzelmüller and Hagen, 2005); or (ii) limited buried ice within the frontal moraine (e.g., Section 4.1). The second scenario is most likely, given the low radar velocities and high signal attenuation found along GPR2, indicative of a debris-rich composition. Similarly, the moraine system at the neighbouring Austre Lovénbreen was found to be debris-rich within frontal zones and ice-rich in lateral zones (Midgley et al., 2013), which has resulted in variable rates of surface change across the moraine system between 2003 and 2014 (Tonkin et al., 2016).

5.3. Influence of glaciofluvial systems and standing water on moraine degradation

Areas with higher rates of surface change (such as on the medial moraine) can most likely be attributed to the development and evolution of glaciofluvial drainage systems, including standing water – both of which represent an important driver of surface change. On debris-covered glaciers, ice cliffs and ponded water are linked to high rates of ablation (e.g., Sakai et al., 2000; Benn et al., 2001, 2012; Juen et al., 2014). In the study by Immerzeel et al. (2014), repeat UAV-derived DEMs were used to measure the evolution of a debris-covered glacier terminus in the Himalaya, showing that 24% of ice-melt could be linked to the presence of supraglacial ponds and ice-cliffs. In this study, glaciofluvial run off was found to incise ice-cored terrain and areas of standing water have developed on the western slope of the medial moraine, resulting in the development of exposed ice-cliffs, which coincide with high rates of surface evolution.

The results contrast with findings at the neighbouring Austre Lovénbreen (Table 2) where repeat SfM DEMs were used to quantify lateral-frontal moraine evolution, highlighting lower rates of surface evolution over the same time period (2003–2014) as this study (Tonkin et al., 2016). The well-drained, elevated position of the ice-cored landforms at Austre Lovénbreen, which are detached from the main glaciofluvial system, were argued to limit the impact of thermo-erosion by run off and standing water, resulting in no exposed ice at the moraine surface. In contrast, glaciofluvial discharge at Midtre

Table 2

A comparison of the vertical rate of moraine degradation quantified in this study with other sites in Svalbard.

Study	Study site	Time period (CE)	Method	Landform – area	Rate of vertical change (ma ⁻¹)
Schomacker and Kjær (2008)	Holmströmbreen	1984–2004	Total station survey	Ice-cored moraine	–0.9
Ewertowski (2014)	Ragnarbreen	1990–2009	Repeat photogrammetric DEMs	Lateral moraine 'End' moraine	–0.08 –0.003
Ewertowski and Tomczyk (2015)	Ragnarbreen and Ebbabreen	2012–2014	Repeat DEMs (Topcon Imaging Station)	Ice-cored moraine (passive down-wastage) Ice-cored moraine (active mass movements)	Up to –0.3 Up to –1.8
Tonkin et al. (2016)	Austre Lovénbreen	2003–2014	Repeat DEMs (SfM photogrammetry)	Lateral-frontal moraine	Variable: e.g. –0.04 to –0.23
Irvine-Fynn et al. (2011)	Midtre Lovénbreen	2003–2005	Repeat DEMs (LiDAR)	'Western lateral moraine' (medial moraine)	–0.65
This study – see Table 1	Midtre Lovénbreen	2003–2014	Repeat DEMs (LiDAR/SfM photogrammetry)	Frontal moraine Medial moraine	–0.09 –0.40

Lovénbreen is routed over ice-cored terrain, resulting in high rates of thermo-erosion. Site-specific characteristics are, therefore, argued to be a highly important control on surface evolution in ice-cored terrain, resulting in the diverse response of high-Arctic glacial landsystems to climatic amelioration. These findings indicate that a diverse response of ice-cored landforms to deglaciation can be anticipated, even for sites with similar glaciological characteristics, or in close proximity to each other. Rates of change on ice-cored moraine appear to be variable, even locally, and represent complex topographic controls on moraine degradation (e.g., Schomacker, 2008).

5.4. Implications of subsurface observations on long-term landscape evolution

Given the strong contrast between the subsurface characteristics detected within the ice-rich zone of GPR1 and the debris-rich zone of GPR1 (where the medial moraine becomes frontal moraine) and along the full length of GPR2, a higher preservation potential of the debris-rich zones is envisaged following complete deglaciation (Fig. 9). However, landscape response to climatic amelioration is dampened by the release of debris from buried ice, which contributes to a thickening surface debris layer that provides underlying ice within greater protection from atmospheric warming (e.g., Østrem, 1959; Nicholson and Benn, 2006). The high debris component in GPR2 may permit zones of stabilised glacier ice within the moraine. However, this is dependent on the relationship

between debris thickness and the response of the active layer to future warming, with permafrost degradation over the twenty-first century principally expected at coastal sites with low elevations (Etzelmüller et al., 2011).

Moraine genesis and degradation rates are also closely linked and require consideration. Medial moraines can develop as the folded limbs of primary stratification and rockfall debris. Material is predominantly transported passively and emerges at the glacier terminus as a thin, linear supraglacial drape of coarse angular debris (Hambrey et al., 1999). In a proglacial setting, the moraines are manifested as linear landforms, oriented parallel to glacier flow, and are volumetrically principally composed of dead/stagnant glacier ice that is typically protected by a thin veneer of sediment (Hambrey and Glasser, 2003). In contrast, the ice content may be more restricted in the frontal moraine, which again, is related to the mode of moraine genesis.

Englacial and proglacial thrusting of subglacial sediment have been discussed as an important moraine-forming process at many high-Arctic glaciers, including Midtre Lovénbreen (Hambrey et al., 1997, 1999; Bennett et al., 1999; Midgley et al., 2007), resulting in a hummocky assemblage of landforms with steep ice-distal slopes and in gentler rectilinear and curvilinear ice-proximal slopes (Glasser and Hambrey, 2003). The long-term preservation potential of such landforms has been debated owing to the potential ice component within the landforms (Lukas, 2005; Graham et al., 2007; Lukas, 2007; Evans, 2009). In the frontal zone, moderate rates of surface lowering are detected overall

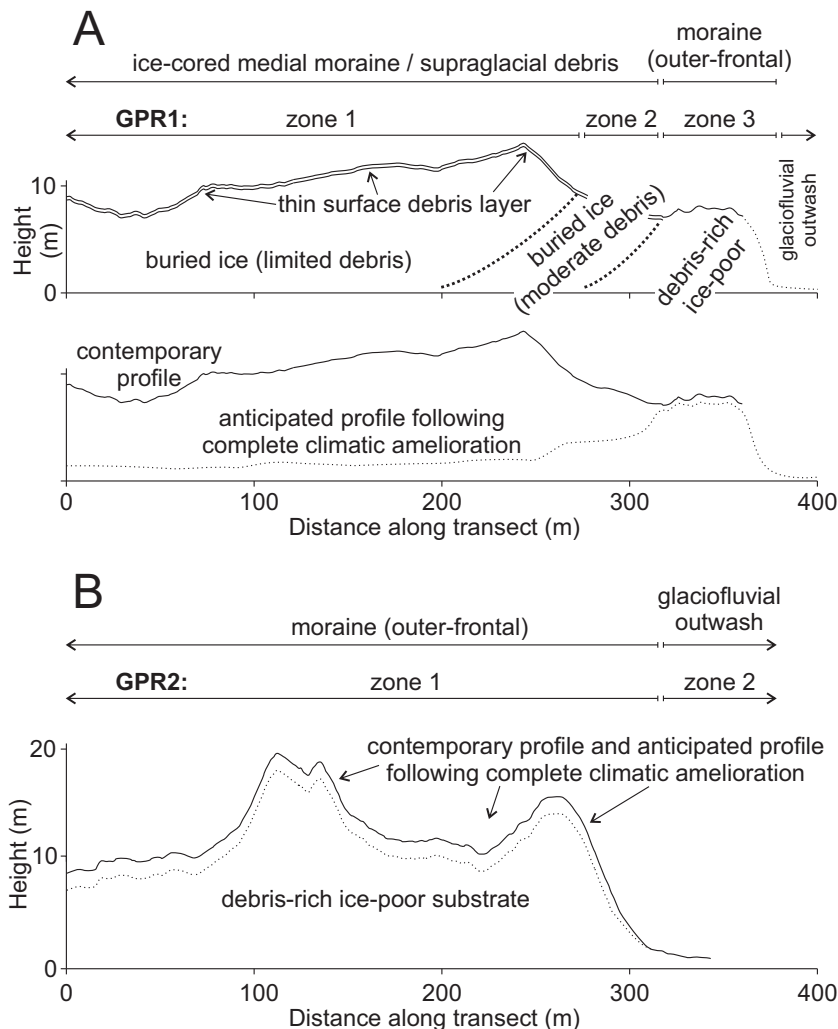


Fig. 9. Schematic model of contemporary moraine and moraine evolution at Midtre Lovénbreen, Svalbard.

(Table 1). Lowering is, however, limited on areas of topographic prominence (e.g., the hummocks; Fig. 7). As structural glaciology and moraine evolution are linked (e.g., Evans, 2009), debris concentrations within stagnant/dead ice exert an important control with regard to landform preservation potential. For example, the Neoglacial ice-margin of Midtre Lovénbreen was near vertical, promoting the flowage of debris emerging at the terminus from a supraglacial to proglacial position (Hambrey, 1894; Hambrey et al., 2005). Such a scenario would result in the development of debris-rich zones within the moraine system. Furthermore, high debris concentrations (e.g., hummocks of glacial sediment) will permit the development of a thick debris mantle to stabilise the landform.

Evans (2009) highlighted that the presence of kettle lakes within the Midtre Lovénbreen proglacial area indicates that ablation of buried ice is occurring. The results of our subsurface characterisation indicate a debris-dominant composition for this Neoglacial frontal moraine. Whilst our results show that the moraine system does appear to be responding to deglaciation, a higher preservation potential is possible as a consequence of the debris-rich subsurface composition. Ultimately, complex debris-rich and ice-rich landform assemblages at adjacent sites (Midgley et al., 2013; Tonkin et al., 2016; this study) highlight the need for care when assessing the palaeoglaciological significance and likely long-term preservation potential of ice-marginal landscapes in the geomorphological record. Appropriate understanding of landform character and landform censoring or degradation history is an important consideration for obtaining appropriate ages for glacial landforms (e.g., Kirkbride and Winkler, 2012; Çiner et al., 2015; Crump et al., 2017; Tonkin et al., 2017) and for glacier reconstructions (e.g., Benn and Hulton, 2010; Pellitero et al., 2016) where moraines are used to constrain the extent and vertical dimensions of former glaciers. As such, a better understanding of this landform type with a mix of debris-rich and ice-rich substrate will prove valuable to assessing age and palaeoclimatic interpretations.

6. Conclusions

The research reported here advances our understanding of the varied ice-debris composition of the proglacial setting and the evolution of proglacial landscape over a decadal timescale in a warming climate. It highlights the complex response of glacial geomorphological systems to climatic change, with spatially variable surface lowering rates detected within and between adjacent glacier forelands; Austre Lovénbreen (Midgley et al., 2013; Tonkin et al., 2016) and the research presented in this study on Midtre Lovénbreen. This study provides insight into the dynamics of a deglaciating high-Arctic landscape over a decadal timescale. Specifically, GPR is used to demonstrate that the composition of ice-marginal landforms is variable. Velocities determined from the GPR surveys demonstrate that the frontal moraine zones of the moraine system are debris-rich (radar velocities of 0.1–0.13 m ns⁻¹), whereas the medial moraine zones are ice-rich (radar velocities of 0.17 m ns⁻¹). The DEM differencing of LiDAR- (2003) and UAV-derived elevation data (2014) are used to quantify landscape response to climatic amelioration. The complex response of the landsystem relates not only to the ice and sediment composition of the landforms but also to the topographic context. The medial moraine zone is undergoing a larger magnitude of change than the frontal and lateral moraine zones as a result of debris thickness and the presence of glaciofluvial drainage and standing water. Site-specific characteristics are, therefore, argued to be a highly important control on surface evolution in ice-cored terrain, with the findings indicating that even at adjacent sites with similar glaciological characteristics, a diverse response of ice-cored landforms to deglaciation can be anticipated. The accessibility of new tools (UAV and SfM) to generate high-resolution topographic data sets is now allowing for the geomorphological response of ice-marginal landsystems to deglaciation to be better understood. A better understanding of contemporary ice-marginal landsystems will assist

with the determination of age and climatic interpretations of the palaeo ice-marginal landsystems that are found in the landform record.

Acknowledgements

The fieldwork was funded by grants from the Royal Society (2007/R2 to DJG and NGM), Nottingham Trent University (NGM and TNT), the Manchester Geographical Society (SJC), and TNT was also in receipt of a Nottingham Trent University VC bursary postgraduate studentship. The winter fieldwork benefited from logistical support provided by Steinar Aksnes at Sverdrup Station (Norwegian Polar Institute) and summer fieldwork benefited from logistical support provided by Nick Cox at Harland Huset (Arctic Office – NERC) with accommodation also provided at Harland Huset during summer fieldwork courtesy of the Arctic Office (NERC). Anya Wicikowski and Lloyd Stanway are thanked for assistance with fieldwork and both received financial support from Nottingham Trent University. The 2003 aerial data are from the UK Natural Environment Research Council (NERC) Airborne Research and Survey Facility (ARSF) that are provided courtesy of NERC via the NERC Earth Observation Data Centre (NEODC). Part of archive aerial photograph S36 1552 from 1936 is published with permission of the Norwegian Polar Institute. A climate data set from the Norwegian Meteorological Institute was downloaded via the eKlima web portal. The reviewers and Richard Marston are thanked for their constructive comments of an earlier version of our manuscript.

Appendix A. Supplementary data

Supplementary data associated with this article can be found in the online version, at <https://doi.org/10.1016/j.geomorph.2018.03.027>. These data include the Google map of the most important areas described in this article.

References

- Arnold, N.S., Rees, W.G., Devereux, B.J., Amable, G.S., 2006. Evaluating the potential of high-resolution airborne LiDAR data in glaciology. *Int. J. Remote Sens.* 27 (6): 1233–1251. <https://doi.org/10.1080/01431160500353817>.
- Ballantyne, C.K., 2002. Paraglacial geomorphology. *Quat. Sci. Rev.* 21 (18–19):1935–2017. [https://doi.org/10.1016/S0277-3791\(02\)00005-7](https://doi.org/10.1016/S0277-3791(02)00005-7).
- Benn, D.I., Hulton, N.R.J., 2010. An Excel™ spreadsheet program for reconstructing the surface profile of former mountain glaciers and ice caps. *Comput. Geosci.* 36 (5): 605–610. <https://doi.org/10.1016/j.cageo.2009.09.016>.
- Benn, D.I., Wiseman, S., Hands, K.A., 2001. Growth and drainage of supraglacial lakes on debris mantled Ngozumpa Glacier, Khumbu Himal, Nepal. *J. Glaciol.* 47 (159): 626–638. <https://doi.org/10.3189/172756501781831729>.
- Benn, D.I., Bolch, T., Hands, K., Gulley, J., Luckman, A., Nicholson, L.I., Quincey, D., Thompson, S., Toumi, R., Wiseman, S., 2012. Response of debris-covered glaciers in the Mount Everest region to recent warming, and implications for outburst flood hazards. *Earth Sci. Rev.* 114:156–174. <https://doi.org/10.1016/j.earscirev.2012.03.008>.
- Bennett, M.R., Huddart, D., Hambrey, M.J., Ghiene, J.F., 1996. Moraine development at the high-arctic valley glacier Pedersenbreen, Svalbard. *Geografiska Annaler, Series A: Physical Geography* 78 (4):209–222. <https://doi.org/10.2307/521041>.
- Bennett, M.R., Hambrey, M.J., Huddart, D., Glasser, N.F., 1998. Glacial thrusting and moraine-mound formation in Svalbard and Britain: the example of Coire a' Cheudchnoic (Valley of Hundred Hills), Torridon Scotland. In: Owen, L.A. (Ed.), *Mountain Glaciation. Quaternary Proceedings* No. 6. John Wiley & Sons Ltd, Chichester, pp. 17–34.
- Bennett, M.R., Hambrey, M.J., Huddart, D., Glasser, N.F., Crawford, K., 1999. The landform and sediment assemblage produced by a tidewater glacier surge in Kongsfjorden, Svalbard. *Quat. Sci. Rev.* 18 (10):1213–1246. [https://doi.org/10.1016/S0277-3791\(98\)90041-5](https://doi.org/10.1016/S0277-3791(98)90041-5).
- Bennett, M.R., Huddart, D., Glasser, N.F., Hambrey, M.J., 2000. Resedimentation of debris on an ice-cored lateral moraine in the high-Arctic (Kongsvegen, Svalbard). *Geomorphology* 35 (1–2):21–40. [https://doi.org/10.1016/S0169-555X\(00\)00017-9](https://doi.org/10.1016/S0169-555X(00)00017-9).
- Bennett, M.R., Huddart, D., Waller, R.I., Cassidy, N., Tomio, A., Zukowskyj, P., Midgley, N.G., Cook, S.J., Gonzalez, S., Glasser, N.F., 2004. Sedimentary and tectonic architecture of a large push moraine: a case study from Hagafellsjökull-Eystrí, Iceland. *Sediment. Geol.* 172 (3–4):269–292. <https://doi.org/10.1016/j.sedgeo.2004.10.002>.
- Bhardwaj, A., Sam, L., Martín-Torres, F.J., Kumar, R., 2016a. UAVs as remote sensing platform in glaciology: present applications and future prospects. *Remote Sens. Environ.* 175:196–204. <https://doi.org/10.1016/j.rse.2015.12.029>.
- Bhardwaj, A., Sam, L., Bhardwaj, A., Martín-Torres, F.J., 2016b. LiDAR remote sensing of the cryosphere: present applications and future prospects. *Remote Sens. Environ.* 177: 125–143. <https://doi.org/10.1016/j.rse.2016.02.031>.

- Björnsson, H., Gjessing, Y., Hamran, S.-E., Hagen, J.O., 1996. The thermal regime of sub-polar glaciers mapped by multi-frequency radio-echo sounding. *J. Glaciol.* 42 (140): 23–32. <https://doi.org/10.3189/S002214300030495>.
- Boulton, G.S., 1972. Modern Arctic glaciers as depositional models for former ice sheets. *J. Geol. Soc.* 128 (4):361–393. <https://doi.org/10.1144/gsjgs.128.4.0361>.
- Brandt, O., Langley, K., Kohler, J., Hamran, S.-E., 2007. Detection of buried ice and sediment layers in permafrost using multi-frequency Ground Penetrating Radar: a case examination on Svalbard. *Remote Sens. Environ.* 111:212–227. <https://doi.org/10.1016/j.rse.2007.03.025>.
- Brasington, J., Langham, J., Rumsby, B., 2003. Methodological sensitivity of morphometric estimates of coarse fluvial sediment transport. *Geomorphology* 53:299–316. [https://doi.org/10.1016/S0169-555X\(02\)00320-3](https://doi.org/10.1016/S0169-555X(02)00320-3).
- Church, M., Ryder, J.M., 1972. Paraglacial sedimentation: a consideration of fluvial processes conditioned by glaciation. *Geol. Soc. Am. Bull.* 83 (10), 3059–3071.
- Çiner, A., Sarıkaya, M.A., Yıldırım, C., 2015. Late Pleistocene piedmont glaciations in the Eastern Mediterranean; insights from cosmogenic ³⁶Cl dating of hummocky moraines in southern Turkey. *Quat. Sci. Rev.* 116:44–56. <https://doi.org/10.1016/j.quascirev.2015.03.017>.
- Crump, S.E., Anderson, L.S., Miller, G.H., Anderson, R.S., 2017. Interpreting exposure ages from ice-cored moraines: a Neoglacial case study on Baffin Island, Arctic Canada. *Boreas* 32 (8):1049–1062. <https://doi.org/10.1002/jqs.2979>.
- Curry, A.M., 1999. Paraglacial modification of slope form. *Earth Surf. Process. Landf.* 24 (13):1213–1228. [https://doi.org/10.1002/\(SICI\)1096-9837\(199912\)24:13<1213::AID-ESP32>3.0.CO;2-B](https://doi.org/10.1002/(SICI)1096-9837(199912)24:13<1213::AID-ESP32>3.0.CO;2-B).
- Curry, A.M., Cleasby, V., Zukowskyj, P., 2006. Paraglacial response of steep, sediment-mantled slopes to post-Little Ice Age glacier recession in the central Swiss Alps. *J. Quat. Sci.* 21 (3):211–225. <https://doi.org/10.1002/jqs.954>.
- De Geer, C., 1930. Flygfärder och polarforskning från Andrée till våra dagar. *Jorden Runt* 2, 577–608.
- Ely, J.C., Graham, C., Barr, I.D., Rea, B.R., Spagnolo, M., Evans, J., 2017. Using UAV acquired photography and structure from motion techniques for studying glacier landforms: application to the glacial flutes at Isfallsgläciären. *Earth Surf. Process. Landf.* 42 (6): 877–888. <https://doi.org/10.1002/esp.4044>.
- Etienne, S., Mercier, D., Voldoire, O., 2008. Temporal scales and deglaciation rhythms in a polar glacier margin, Barónbreen, Svalbard. *Nor. Geogr. Tidsskr.* 62 (2):102–114. <https://doi.org/10.1080/00291950802095111>.
- Etzelmüller, B., Hagen, J.O., 2005. Glacier-permafrost interaction in Arctic and alpine mountain environments with examples from southern Norway and Svalbard. In: Harris, C., Murton, J. (Eds.), *Cryospheric Systems – Glaciers and Permafrost*. The Geological Society of London, Special Publications 242:pp. 11–27. <https://doi.org/10.1144/GSL.SP.2005.242.01.02>.
- Etzelmüller, B., Schuler, T.V., Isaksen, K., Christiansen, H.H., Farbrøt, H., Benestad, R., 2011. Modeling the temperature evolution of Svalbard permafrost during the 20th and 21st century. *Cryosphere* 5 (1):67–79. <https://doi.org/10.5194/tc-5-67-2011>.
- Evans, D.J.A., 2009. Controlled moraines: origins, characteristics and palaeogeological implications. *Quat. Sci. Rev.* 28 (3–4):183–208. <https://doi.org/10.1016/j.quascirev.2008.10.024>.
- Ewertowski, M., 2014. Recent transformations in the high-Arctic glacier landscape, Ragnarbreen, Svalbard. *Geografiska Annaler: Series A (Physical Geography)* 96: 265–285. <https://doi.org/10.1111/geoa.12049>.
- Ewertowski, M., Tomczyk, A.M., 2015. Quantification of the ice-cored moraines' short-term dynamics in the high-Arctic glaciers Ebbabreen and Ragnarbreen, Petuniabukta, Svalbard. *Geomorphology* 234:211–227. <https://doi.org/10.1016/j.geomorph.2015.01.023>.
- Fame, M.L., Owen, L.A., Spotila, J.A., Dortch, J.M., Caffee, M.W., 2018. Tracking paraglacial sediment with cosmogenic ¹⁰Be using an example from the northwest Scottish Highlands. *Quat. Sci. Rev.* 182:20–36. <https://doi.org/10.1016/j.quascirev.2017.12.017>.
- Fitzsimons, S.J., 1996. Paraglacial redistribution of glacial sediments in the Vestfold Hills, East Antarctica. *Geomorphology* 15 (2), 93–108.
- Førland, E.J., Benestad, R., Hanssen-Bauer, I., Haugen, J.E., Skaugen, T.E., 2011. Temperature and precipitation development at Svalbard 1900–2100. *Adv. Meteorol.* 893790. <https://doi.org/10.1155/2011/893790>.
- Glasser, N.F., Hambrey, M.J., 2003. Ice-marginal terrestrial land systems: Svalbard polythermal glaciers. In: Evans, D.J.A. (Ed.), *Glacial Land Systems*. Arnold, London, pp. 65–88.
- Graham, D.J., Midgley, N.G., 2000. Moraine-mound formation by englacial thrusting: the Younger Dryas moraines of Cwm Idwal, North Wales. In: Maltman, A.J., Hubbard, B., Hambrey, M.J. (Eds.), *Deformation of Glacial Materials*. The Geological Society of London, Special Publications 176, pp. 321–336.
- Graham, D.J., Bennett, M.R., Glasser, N.F., Hambrey, M.J., Huddart, D., Midgley, N.G., 2007. 'A test of the englacial thrusting hypothesis of "hummocky" moraine formation: case studies from the northwest Highlands, Scotland'. *Comments. Boreas* 36 (1):103–107. <https://doi.org/10.1111/j.1502-3885.2007.tb01184.x>.
- Hamberg, A., 1894. En resa till norra Ishafvet sommaren 1892. *Ymer* 14, 25–61.
- Hambrey, M.J., Glasser, N.F., 2003. The role of folding and foliation development in the genesis of medial moraines: examples from Svalbard glaciers. *The Journal of Geology* 111 (4):471–485. <https://doi.org/10.1086/375281>.
- Hambrey, M.J., Huddart, D., Bennett, M.R., Glasser, N.F., 1997. Genesis of "hummocky moraines" by thrusting in glacier ice: evidence from Svalbard and Britain. *J. Geol. Soc.* 154:623–632. <https://doi.org/10.1144/gsjgs.154.4.0623>.
- Hambrey, M.J., Bennett, M.R., Dowdeswell, J.A., Glasser, N.F., Huddart, D., 1999. Debris entrainment and transfer in polythermal valley glaciers. *J. Glaciol.* 45 (149):69–86. <https://doi.org/10.3189/1999jg45-149-69-86>.
- Hambrey, M.J., Murray, T., Glasser, N.F., Hubbard, A., Hubbard, B., Stuart, G., Hansen, S., Kohler, J., 2005. Structure and changing dynamics of a polythermal valley glacier on a centennial time-scale: Midre Lovénbreen, Svalbard. *J. Geophys. Res. Earth Surf.* F010006. <https://doi.org/10.1029/2004JF000128>.
- Hanoa, R., 1993. *Kings Bay Kull Comp. A/S 1917–1992: fra gruvedrift til forskningservice på Svalbard*. Oslo, Schibsted (245 pp.).
- Immerzeel, W.W., Kraaijenbrink, P.D.A., Shea, J.M., Shrestha, A.B., Pellicciotti, F., Bierkens, M.F.P., De Jong, S.M., 2014. High-resolution monitoring of Himalayan glacier dynamics using unmanned aerial vehicles. *Remote Sens. Environ.* 150:93–103. <https://doi.org/10.1016/j.rse.2014.04.025>.
- Irvine-Fynn, T.D.L., Barrand, N.E., Porter, P.R., Hodson, A.J., Murray, T., 2011. Recent High-Arctic glacial sediment redistribution: a process perspective using airborne lidar. *Geomorphology* 125 (1):27–39. <https://doi.org/10.1016/j.geomorph.2010.08.012>.
- Isachsen, G., 1912. *Exploration du Nord-Ouest du Spitsberg entreprise sous les auspices de S.A.S. le Prince de Monaco par la Mission Isachsen*, Fascicule XL, Imprimerie de Monaco.
- Juen, M., Mayer, C., Lambrecht, A., Han, H., Liu, S., 2014. Impact of varying debris cover thickness on ablation: a case study for Koxkar Glacier in the Tien Shan. *Cryosphere* 8 (2):377–386. <https://doi.org/10.5194/tc-8-377-2014>.
- Kirkbride, M.P., Winkler, S., 2012. Correlation of Late Quaternary moraines: impact of climate variability, glacier response, and chronological resolution. *Quat. Sci. Rev.* 46: 1–29. <https://doi.org/10.1016/j.quascirev.2012.04.002>.
- Knight, J., Harrison, S., 2009. Periglacial and paraglacial environments: a view from the past into the future. In: Knight, J., Harrison, S. (Eds.), *Periglacial and Paraglacial Processes and Environments*. Geological Society, London, Special Publications 320: pp. 1–4. <https://doi.org/10.1144/SP320.1>.
- Lønne, I., Lyså, A., 2005. Deglaciation dynamics following the Little Ice Age on Svalbard: implications for shaping of landscapes at high latitudes. *Geomorphology* 72 (1): 300–319. <https://doi.org/10.1016/j.geomorph.2005.06.003>.
- Lukas, S., 2005. A test of the englacial thrusting hypothesis of 'hummocky' moraine formation: case studies from the northwest Highlands, Scotland. *Boreas* 34 (3):287–307. <https://doi.org/10.1111/j.1502-3885.2005.tb01102.x>.
- Lukas, S., 2007. 'A test of the englacial thrusting hypothesis of "hummocky" moraine formation: case studies from the northwest Highlands, Scotland': reply to comments. *Boreas* 36 (1):108–113. <https://doi.org/10.1111/j.1502-3885.2007.tb01185.x>.
- Lukas, S., Sass, O., 2011. The formation of Alpine lateral moraines inferred from sedimentology and radar reflection patterns: a case study from Gomerletscher, Switzerland. *Geol. Soc. Lond. Spec. Publ.* 354, 77–92.
- Lyså, A., Lønne, I., 2001. Moraine development at a small High-Arctic valley glacier: Rieperbreen, Svalbard. *J. Quat. Sci.* 16 (6):519–529. <https://doi.org/10.1002/jqs.613>.
- Martin-Moreno, R., Allende Álvarez, F., Hagen, J.O., 2017. Little Ice Age glacier extent and subsequent retreat in Svalbard archipelago. *The Holocene* 27 (9):1–12. <https://doi.org/10.1177/0959683617693904>.
- Mercier, D., Etienne, S., Sellier, D., André, M.-F., 2009. Paraglacial gullying of sediment-mantled slopes: a case study of Colletthøgda, Kongsfjorden area, West Spitsbergen (Svalbard). *Earth Surf. Process. Landf.* 34 (13):1772–1789. <https://doi.org/10.1002/esp.1862>.
- Midgley, N.G., Tonkin, T.N., 2017. Reconstruction of former glacier surface topography from archive oblique aerial images. *Geomorphology* 282:18–26. <https://doi.org/10.1016/j.geomorph.2017.01.008>.
- Midgley, N.G., Glasser, N.F., Hambrey, M.J., 2007. Sedimentology, structural characteristics and morphology of a Neoglacial high-Arctic moraine-mound complex: Midre Lovénbreen, Svalbard. In: Hambrey, M.J., Christoffersen, P., Glasser, N.F., Hubbard, B. (Eds.), *Glacial Sedimentary Processes and Products*, International Association of Sedimentologists, Special Publication 39:pp. 11–23. <https://doi.org/10.1002/9781444304435.ch2>.
- Midgley, N.G., Cook, S.J., Graham, D.J., Tonkin, T.N., 2013. Origin, evolution and dynamic context of a Neoglacial lateral-frontal moraine at Austre Lovénbreen, Svalbard. *Geomorphology* 198:96–106. <https://doi.org/10.1016/j.geomorph.2013.05.017>.
- Murton, J.B., Whiteman, C.A., Waller, R.L., Pollard, W.H., Clark, I.D., Dallimore, S.R., 2005. Basal ice facies and supraglacial melt-out till of the Laurentide Ice Sheet, Tuktoyaktuk Coastlands, western Arctic Canada. *Quat. Sci. Rev.* 24 (5–6):681–708. <https://doi.org/10.1016/j.quascirev.2004.06.008>.
- Nicholson, L., Benn, D.I., 2006. Calculating ice melt beneath a debris layer using meteorological data. *J. Glaciol.* 52 (178):463–470. <https://doi.org/10.3189/172756506781828584>.
- Norwegian Polar Institute, 2014. Kartdata Svalbard 1:100,000 (S100 Kartdata). Norwegian Polar Institute, Tromsø, Norway Available at: <https://data.npolar.no/dataset/645336c7-adfe-4d5a-978d-9426fe788ee3>.
- Oliva, M., Ruiz-Fernández, J., 2015. Coupling patterns between para-glacial and permafrost degradation responses in Antarctica. *Earth Surf. Process. Landf.* 40 (9), 1227–1238.
- Østrem, G., 1959. Ice melting under a thin layer of moraine, and the existence of ice cores in moraine ridges. *Geogr. Ann.* 41 (4), 228–230.
- Osuch, M., Wawrzyniak, T., 2017. Inter- and intra-annual changes in air temperature and precipitation in western Spitsbergen. *Int. J. Climatol.* 37:3082–3097. <https://doi.org/10.1002/joc.4901>.
- Pellitero, R., Rea, B.R., Spagnolo, M., Bakke, J., Ivy-Ochs, S., Frew, C.R., Hughes, P., Ribolini, A., Lukas, S., Renssen, H., 2016. GlaRe, a GIS tool to reconstruct the 3D surface of palaeoglaciers. *Comput. Geosci.* 94:77–85. <https://doi.org/10.1016/j.cageo.2016.06.008>.
- Rippin, D.M., Pomfret, A., King, N., 2015. High resolution mapping of supra-glacial drainage pathways reveals link between micro-channel drainage density, surface roughness and surface reflectance. *Earth Surf. Process. Landf.* 40 (10):1279–1290. <https://doi.org/10.1002/esp.3719>.
- Rossini, M., Di Mauro, B., Garzonio, R., Baccolo, G., Cavallini, G., Mattavelli, M., De Amicis, M., Colombo, R., 2018. Rapid melting dynamics of an alpine glacier with repeated UAV photogrammetry. *Geomorphology* 304:159–172. <https://doi.org/10.1016/j.geomorph.2017.12.039>.
- Sakai, A., Takeuchi, N., Fujita, K., Nakawo, M., 2000. Role of supraglacial ponds in the ablation process of a debris-covered glacier in the Nepal Himalayas. *IAHS Publ.* 119–132.

- Schäfer, J.M., Heinrich, B., Denton, G.H., Ivy-Ochs, S., Marchant, D.R., Schlüchter, C., Rainer, W., 2000. The oldest ice on Earth in Beacon Valley, Antarctica: new evidence from surface exposure dating. *Earth Planet. Sci. Lett.* 179 (1):91–99. [https://doi.org/10.1016/S0012-821X\(00\)00095-9](https://doi.org/10.1016/S0012-821X(00)00095-9).
- Schomacker, A., 2008. What controls dead-ice melting under different climate conditions? A discussion. *Earth Sci. Rev.* 90 (3–4):103–113. <https://doi.org/10.1016/j.earscirev.2008.08.003>.
- Schomacker, A., Kjær, K.H., 2008. Quantification of dead-ice melting in ice-cored moraines at the high-Arctic glacier Holmstrombreen, Svalbard. *Boreas* 37:211–225. <https://doi.org/10.1111/j.1502-3885.2007.00014.x>.
- Sharp, M., 1984. Annual moraine ridges at Skálafellsjökull, south-east Iceland. *J. Glaciol.* 30 (104):82–93. <https://doi.org/10.3189/S0022143000008522>.
- Sletten, K., Lyså, A., Lønne, I., 2001. Formation and disintegration of a high-arctic ice-cored moraine complex, Scott Turnerbreen, Svalbard. *Boreas* 30 (4):272–284. <https://doi.org/10.1111/j.1502-3885.2001.tb01046.x>.
- Sugden, D.E., Marchant, D.R., Potter Jr., N., Souchez, R.A., Denton, G.H., Swischer III, C.C., Tison, J.-L., 1995. Preservation of Miocene glacier ice in east Antarctica. *Nature* 376:412–414. <https://doi.org/10.1038/376412a0>.
- Tonkin, T.N., Midgley, N.G., 2016. Ground-control networks for image based surface reconstruction: an investigation of optimum survey designs using UAV derived imagery and Structure-from-Motion photogrammetry. *Remote Sens.* 8 (9):786. <https://doi.org/10.3390/rs8090786>.
- Tonkin, T.N., Midgley, N.G., Graham, D.J., Labadz, J.C., 2014. The potential of small unmanned aircraft systems and structure-from-motion for topographic surveys: a test of emerging integrated approaches at Cwm Idwal, North Wales. *Geomorphology* 226:35–43. <https://doi.org/10.1016/j.geomorph.2015.12.019>.
- Tonkin, T.N., Midgley, N.G., Cook, S.J., Graham, D.J., 2016. Ice-cored moraine degradation mapped and quantified using an unmanned aerial vehicle: a case study from a polythermal glacier in Svalbard. *Geomorphology* 258:1–10. <https://doi.org/10.1016/j.geomorph.2015.12.019>.
- Tonkin, T.N., Midgley, N.G., Labadz, J.C., Graham, D.J., 2017. Internal structure and significance of ice-marginal moraine in the Kebnekaise Mountains, northern Sweden. *Boreas* 46 (2):199–211. <https://doi.org/10.1111/bor.12220>.
- Toubes-Rodrigo, M., Cook, S.J., Elliott, D., Sen, R., 2016. Sampling and describing glacier ice. In: Cook, S.J., Clarke, L.E., Nield, J.M. (Eds.), *Geomorphological Techniques (Online Edition)*. British Society for Geomorphology, London, UK.
- Waller, R.L., Murton, J.B., Kristensen, L., 2012. Glacier–permafrost interactions: processes, products and glaciological implications. *Sediment. Geol.* 255–256:1–28. <https://doi.org/10.1016/j.sedgeo.2012.02.005>.
- WGMS, 2017. In: Zemp, M., Nussbaumer, S.U., Gärtner-Roer, I., Huber, J., Machguth, H., Paul, F., Hoelzle, M. (Eds.), *Global Glacier Change Bulletin No. 2 (2014–2015)*. ICSU (WDS)/IUGG (IACS)/UNEP/UNESCO/WMO, World Glacier Monitoring Service, Zurich, Switzerland <https://doi.org/10.5904/wgms-fog-2017-10> (244 pp.).
- Wheaton, J.M., Brasington, J., Darby, S.E., Sear, D.A., 2010. Accounting for uncertainty in DEMs from repeat topographic surveys: improved sediment budgets. *Earth Surf. Process. Landf.* 35 (2):136–156. <https://doi.org/10.1002/esp.1886>.